37. Analysis of Coherent Microwave Photonic Filter for Digital Modulation Scheme

Tanooja Mishra[(1)] , Abhinav Gautam[(1)] , Amitesh Kumar[(1)]
[(1)] Department of Electronics Engineering, Indian Institute of Technology (ISM), Dhanbad.
**Corresponding author's e-mail address: sci.tanoojamishra018@gmail.com*

ABSTRACT

Coherent Microwave Photonic Filters (MPFs) are widely discovered for their ability to filter-out high-frequency microwave signals. In this paper, the analysis of a coherent MPF has been carried out for digital data communication using the OptiSystem simulation software. Eye-diagram, constellation diagram, and Probability of Error (PoE) have been investigated for the characterization of MPF using 8-DPSK and 64-QAM digital modulation schemes. The PoE in received signal is calculated for various optical fiber lengths at digital data rate 3 Gbps. Therefore, this analysis would be useful for next generation 5G communication by choosing the appropriate modulation scheme and observing various parameters such as Eye-diagram, constellation diagram, and PoE.

Index Terms— *Digital modulation Schemes (8-DPSK and 64QAM); Microwave photonic filter; Probability of Error; Eyediagram; Constellation diagram.*

INTRODUCTION

In the recent decade, the multidisciplinary area Microwave Photonics (MWPs) is a prominent area of research which offers the simultaneous study of optical and microwave signal in the same platform. Because of its unique characteristics, such as realization of delay lines for signal processing [1], ability to handling of phase and amplitude of a signal independently [2], center frequency tunability, etc., MWP has opened door for [wide range of applications. These applications are in the field of defense, RADAR, optical communication, photonic sensing, MWP filters, Fiber-to-Home or radio over fiber, etc.

In fact, new interdisciplinary technology has been adopted for the interface between microwave engineering and photonics in the optical domain to filter out high-frequency microwave signal, which is commonly known as Microwave Photonic Filters (MPFs). It facilitates the opting of desired frequency from the microwave signals through the processing of optical signals and therefore, paid significant contribution in the radar monitoring, prediction of unknown frequency, defense and military. At high-frequency microwave signals, these filters eliminate the difficulty of higher heat generation and other frequency-dependent losses with conventional electrical microwave filters and work efficiently [3], [4], [5]. Incoherent MPF is implemented using delay lines under FIR or IIR configuration. The incoherent light source is used for suppressing optical interference while using the incoherent MPFs, whereas coherent MPF is realized by using a single wavelength light source without any delay line configurations.

Also, there is no such issue of optical interference in the coherent MPF [6]. It possesses its application in nextgeneration 5G communication. Now a days, the demand for high data rates, service quality, and high bandwidth of transmission media has been increased due to increasing number of users in wireless network [7]. This next generation 5G communication works in millimeter-wave frequency range from 30 GHz to 300 GHz. It offers high bandwidth, high speed transmission of multi Gbps data, and also provides space for wireless monitoring through sensing network and smart city initiatives [8], [9]. Also, huge wireless transportation is possible in 5G communication. For this purpose, high-frequency RF signals are utilized for high speed data transmission. However, there is a problem to filter out these high-frequency RF signals using conventional electrical filters. Therefore MPFs are considered. In this manuscript, a simple, coherent MPF based on an optical Fabry Perot Filter (FPF) is proposed. Also, the analysis of MPF is done for different digital modulation schemes.

Digital modulation schemes offer higher security of data, extra information capacity, and obtainability of high speed system with excessive-quality of communication. Also, digital modulation schemes transfer higher amounts of data in compare to analog modulation schemes. Therefore, in communication systems, digital modulation schemes are most commonly used. Where, high-frequency carrier signal will get modulated through binary digital data that is imposed through varying amplitude, varying phase, and frequency of carrier signal. Now a days, Different types of modulations such as Binary Phase Shift Keying (BPSK), Quadrature Amplitude Modulation (QAM), M-ary Differential Phase Shift Keying (M-DPSK), Mary, PSK (M-PSK), and Quadrature Phase Shift Keying (QPSK), etc. are used. M-DPSK is an effective bandwidth digital modulation scheme and broadly used in mobile radio where the partial radio bandwidth is available [10]. Whereas, for high-capacity of transmission links, M-QAM having high spectral efficiency of optical signals can be generally deployed [11]. As the order of modulation schemes increases, the number of bits per symbol are also increasing, and bandwidth has been effectively utilized. Here, 8-DPSK (3 bit per symbol) and 64QAM (6 bit per symbol) modulation schemes are used.

In this manuscript, section 2 gives the brief overview of block diagram of proposed MPF. Section 3 provides a detailed analysis of proposed coherent MPF where the quality of demodulated data is examined on the basis of constellation diagram, eye-diagram, and PoE.

THEORY

Thes chematic block diagram of the proposed coherent MPF has been shown in Fig.37-1. This proposed MPF consists of a Mach-Zehnder Modulator (MZM) as a Phase Modulator (PM), an optical source, a Photo Detector (PD), and a bandpass filter using an optical Fabry Perot Filter (FPF). Here, an optical FPF is an essential element of coherent MPF. A laser source is used to generate a high-frequency optical carrier signal. An optical carrier signal is incident to MZM, which modulates it by a Radio Frequency (RF) signal that carries digital data. A Pseudo Random Bit Sequence (PRBS) is taken as digital data at rate of 3 Gbps for different digital modulation schemes.

In this analysis, 8-DPSK and 64-QAM digital modulation schemes are used to analyse the performance of coherent MPF. At the output of MZM, an intensity modulated signal is obtained, which consists of optical carrier, upper and lower sidebands. The intensity modulated signal is passed through the FPF to filter out undesired sidebands by selecting a particular Free Spectral Range (FSR). At the output of FPF, an optical carrier signal and first-order upper sideband are obtained. This optical carrier signal and first-order upper sideband beat upon PD. An RF signal is generated at the output of PD. An electrical amplifier is used to amplify RF signal. After amplification process, an RF signal is demodulated using 8-DPSK and 64QAM digital demodulation schemes. Thus, A digital data is successfully recovered. Further, the received digital data is analysed on the basis of probability of error, eye diagram, and constellation diagram.

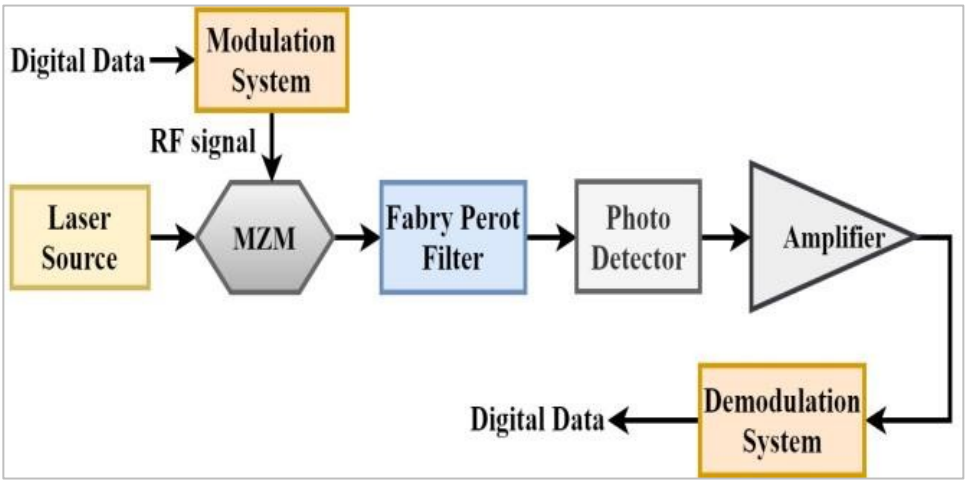

Figure 37-1 Block diagram of coherent microwave photonic filter

SIMULATION EXPERIMENT AND RESULTS

The experimental setup is conducted and simulated on the commercial OptiSystem simulation software platform. The filter response of proposed coherent MPF based on FPF is analysed. Fig.37-2 shows the filter response for sweeping range of frequency from 0 to 60 GHz of proposed coherent MPF. In this figure, it can be observed that the filter gives high-frequency response at only 30 GHz frequency apart from this frequency; the power will be degraded. The bandwidth of FPF is 0.1 GHz, and FSR is 30 GHz. The proposed coherent MPF filter is tuned at 30 GHz frequency. It works as bandpass filter.

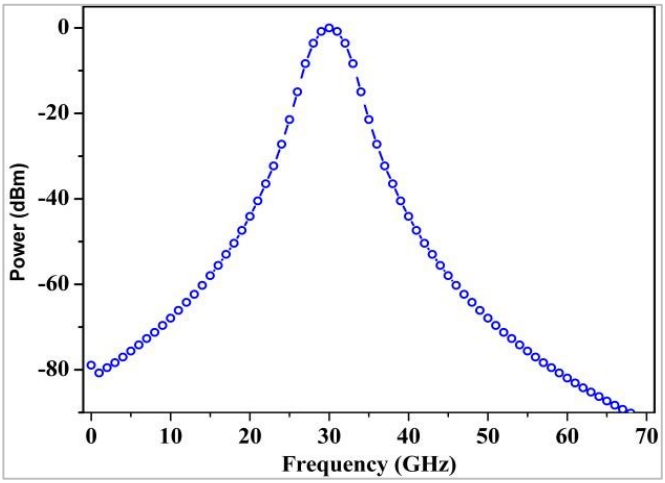

Figure 37-2 Filter Response of Fabry Perot Filter.

Fig.37-3 shows the schematic diagram of modulation system. Where, initially, a PRBS is generated at data rate 3 Gbps by using a periodic pseudo random sequence generator and converted into two bit sequences, i.e., in-phase (I) and quadrature-phase (Q) sequence using 8-DPSK and 64-QAM sequence generator. Further, I and Q bit sequences are applied to two different M-ary pulse generator and converted into two

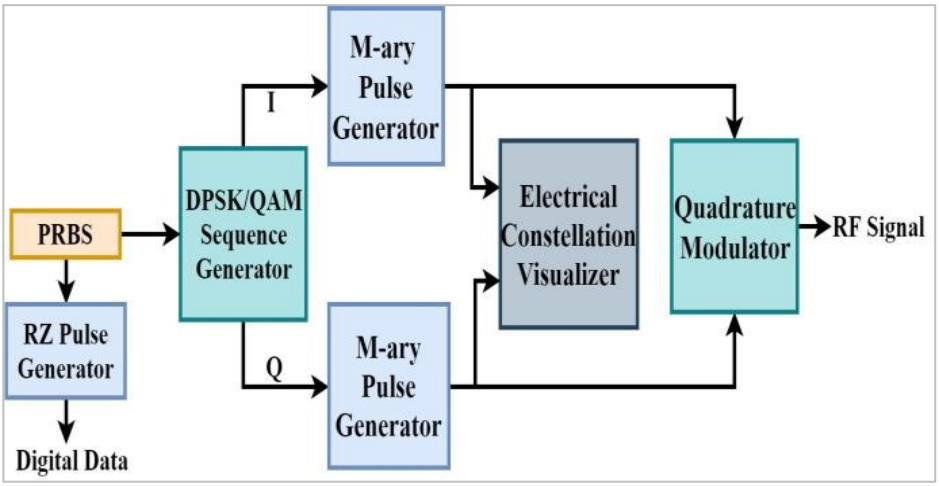

Figure 37-3 Schematic diagram of modulation system.

M-ary pulse form. A constellation diagram which shows digital modulated signal for 8-DPSK and 64-QAM digital modulation scheme, as shown in Fig. 37-4, is obtained using an electrical constellation visualizer that is connected between two M-ary pulse generator.

I and Q M-ary pulse waveforms are transferred and get modulated at high frequency 30 GHz using quadrature modulator. A RF signal is generated at 30 GHz and transmitted through wireless media. At receiver end, the RF

signal is received at antenna and used as a modulating signal that modulates an optical carrier signal at frequency 193.1 THz using MZM. An intensity modulated signal is obtained at the output terminal of MZM, which is shown in Fig.37-4.

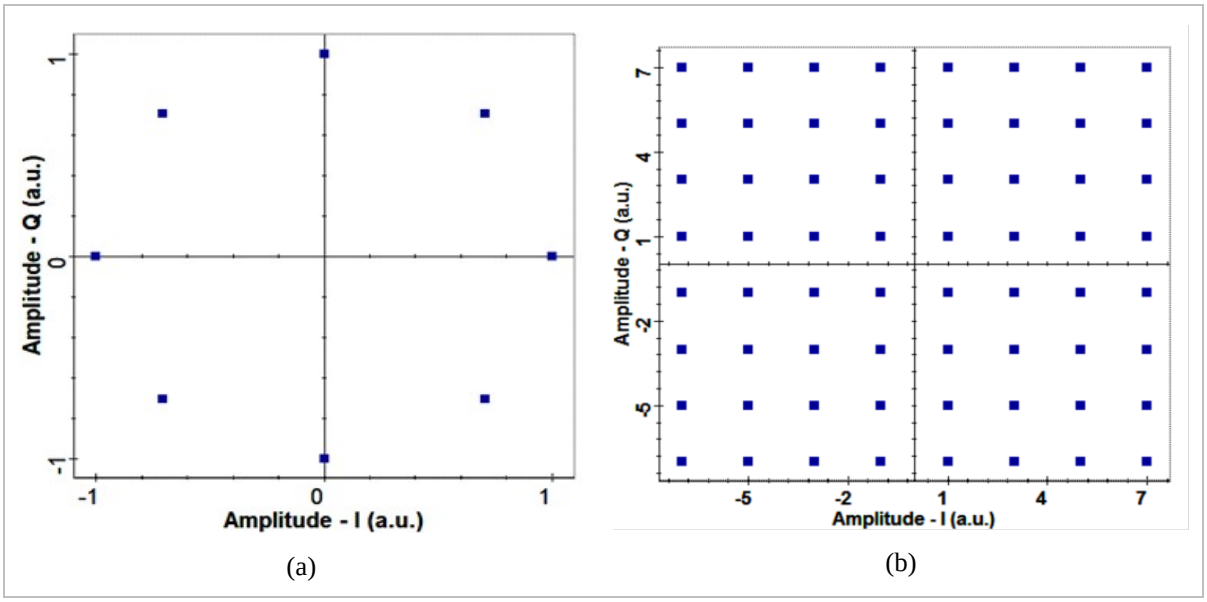

Figure 37-4 Ideal constellation diagram at input for (a) 8-DPSK and (b) 64QAM

Fig. 37-5 depicts an optical carrier signal, upper and lower sidebands. The optical carrier signal at frequency 193.1 THz and upper sideband at frequency 193.13 THz or adjacent sidebands are separated by 30 GHz frequency same as an RF signal frequency. Therefore, an intensity modulated signal is passed through an FPF that is tuned at 193.1 with Free Spectral Range (FSR) of 30 GHz frequency. An optical carrier and upper sideband are beaten upon a PD, and an electrical RF signal at 30 GHz frequency is observed. The received RF signal gets amplified by an electrical amplifier.

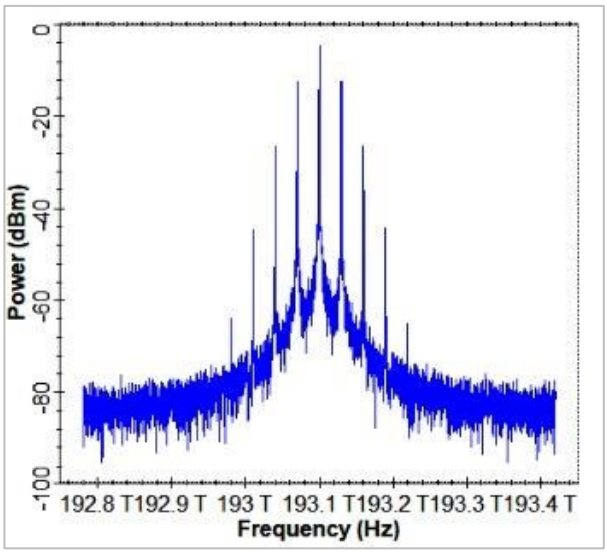

Figure 37-5 An intensity modulated signal at MZM output.

Fig. 37-6 shows schematic diagram of demodulation system. Further, a received RF signal is demodulated and converted into I and Q electrical signal using quadrature demodulator. Furthermore, I and Q waveform are applied to different M-ary threshold detector that approximates signal to desired threshold level. An electrical

constellation visualizer is connected between different M-ary threshold detector to observe the constellation diagrams of received signal using 8-DPSK and 64-QAM digital modulation scheme, as shown in Fig. 37-7.

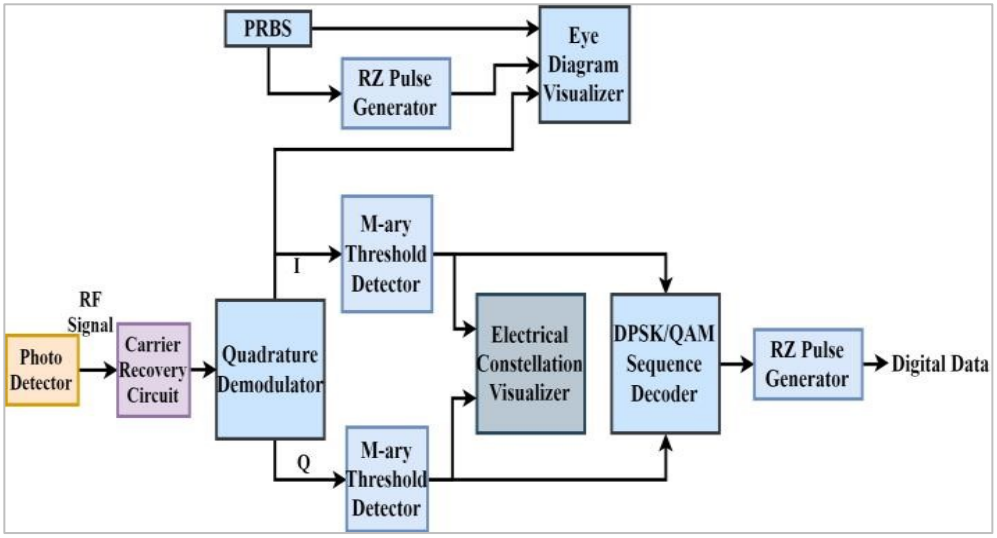

Figure 37-6 Schematic diagram of demodulation system.

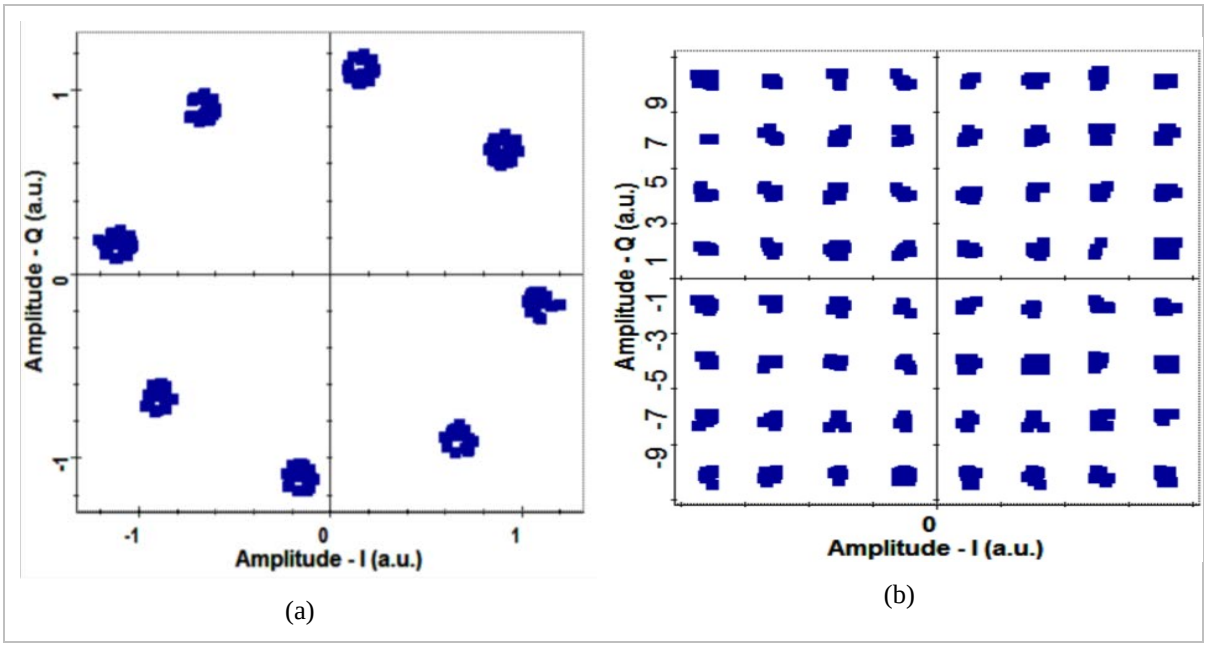

Figure 37-7 Constellation diagram at output for (a) 8-DPSK and (b) 64-QAM

Because of noise added in received signal, the symbol points have been shifted from their ideal coded value. After detecting an RF electrical signal, a channel recovery circuit is required for minimizing error at receiver end for demodulating of digital data. Due to large carrier-frequency offsets and optical noise, large phase errors are introduced in received signal, that can also be tolerated [12]. Carrier recovery circuit estimates and compensates the phase offset of the signal, and the frequency offset between the Local Oscillator (LO) and the signal [13].

However, some noise factors are remaining present in demodulated signal, which cannot be removed using carrier recovery circuit. Therefore, an ideal constellation diagram could not be recovered at receiver end. 8-DPSK has less symbol errors in compare to 64-QAM because of larger distance between adjacent symbol points in I and Q plane. Moreover, the outputs of different M-ary threshold detector are decoded using 8-DPSK and 64-QAM

sequence decoder. After decoding of signal, a RZ pulse generator is used to convert decoded data into electrical pulse form. A digital input data is effectively recovered at 3 Gbps data rate.

The performance of the system is evaluated by measuring an essential factor known as eye-diagram. At the output of quadrature modulator, an eye-diagram of received in-phase Mary signal for 8-DPSK and 64-QAM is obtained by using an eye-diagram visualizer tool, which is shown in Fig. 37-8. By observing eye-diagram, the presence of Inter-Symbol Interference (ISI) which limits signal to noise ratio, and quality of recovered digital data can be determined in high speed digital transmission.

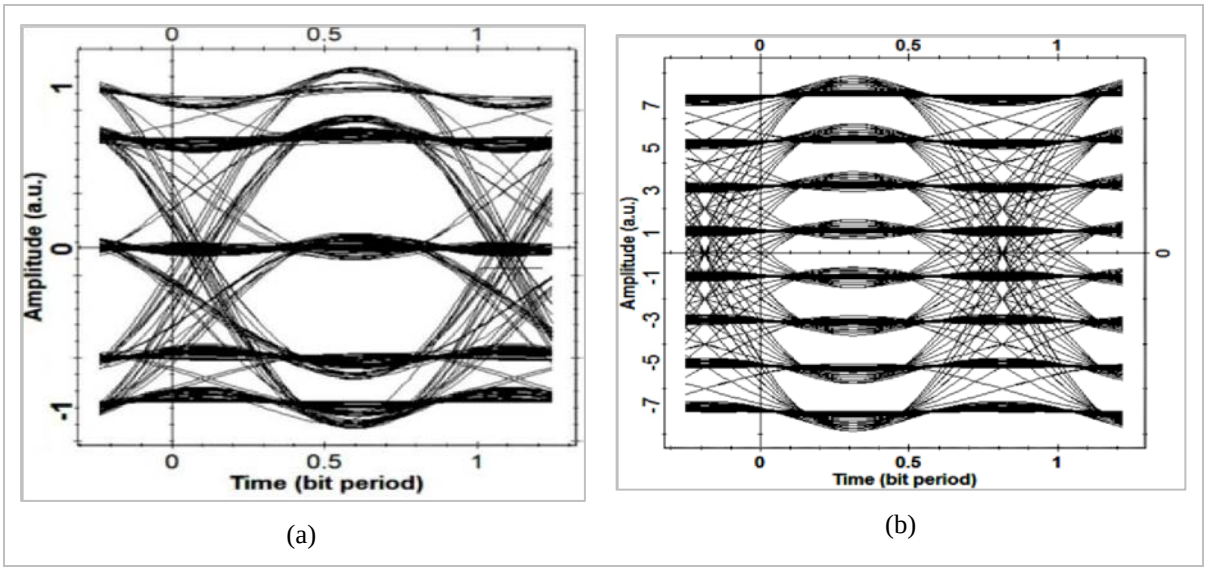

Figure 37-8 Eye diagram of received signal for (a) 8-DPSK and (b) 64-QAM

The eye opening for 8-DPSK signal is larger than 64-QAM because of more ISI existing in 64-QAM signal. But, whenever the data rate starts to increase, the opening of eye-diagram for 8-DPSK tends to decrease and become lesser than 64-QAM, which will still remain the same. Therefore, 64-QAM performs better and gives better results than 8-DPSK for higher data rate [14][15].

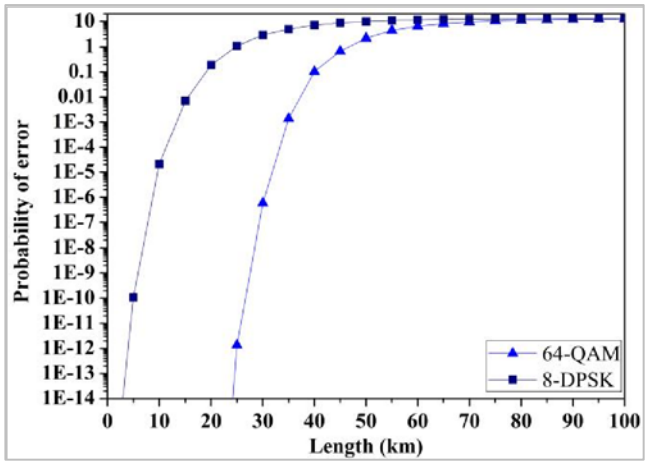

Figure 37-9 Probability of error vs. received power

Another important parameter, i.e., Probability of Error (PoE) of demodulated digital data, is investigated to characterize the performance of digital communication system. In this manuscript, the performance of coherent MPF has been examined for various optical fiber lengths. The Fig. 37-9 shows that the PoE is continuously changing as the optical fiber length is varying from 0 to 100 Km for both modulation scheme 8DPSK and 64-

QAM. PoE should be as low as possible so that the performance of system will be better. Hence, from this graph, it can be depicted that for 64-QAM, the PoE starts to increase from 10^{-9} after 29 Km length of optical fiber. However, for 8-DPSK, the PoE starts to increase from 10^{-9} after 8 Km length of optical fiber. Generally, the acceptable PoE is in the range of 10^{-9} or lower than this value. It is considered as optimum PoE in digital communication system. For larger distance and higher data rate, 64-QAM is preferred. This simulation experiment of coherent MPF is analyzed and justified for digital communication. This examination of analysis of coherent MPF will be useful in next generation 5G communication setup.

CONCLUSION

The simulation analysis of coherent microwave photonic filter has been analysed for different digital modulation scheme through the OptiSystem simulation software. Furthermore, 8-DPSK and 64-QAM digital modulation and demodulation schemes has been investigated in which it has been found that 64-QAM offers better performance than 8-DPSK scheme. Also, different parameters such as constellation diagram, eyediagram, and probability of error has been investigated, which indicated that the 64-QAM would be more suitable for the optical communication, like, 5G optical communication than 8DPSK.

REFERENCES

[1] R. A. Minasian, “Photonic signal processing of microwave signals,” IEEE Transactions on Microwave Theory and Techniques, vol. 54, no. 2, pp. 832–846, Feb. 2006.

[2] J. Yao, “Microwave Photonics,” Journal of Lightwave Technology, vol. 27, no. 3, pp. 314–335, Feb. 2009.

[3] R. J. Cameron, C. M. Kudsia, and R. R. Mansour, Microwave filters for communication systems: Fundamentals, design, and applications. 2018.

[4] J. Capmany, B. Ortega, and D. Pastor, “A tutorial on microwave photonic filters,” Journal of Lightwave Technology, 2006.

[5] J. Capmany, B. Ortega, D. Pastor, and S. Sales, “Discrete-time optical processing of microwave signals,” Journal of Lightwave Technology, 2005.

[6] J. Yao, “Photonics to the Rescue: A Fresh Look at Microwave Photonic Filters,” IEEE Microwave Magazine, 2015.

[7] R. M. Aly, A. Zaki, W. K. Badawi, and M. H. Aly, “Time coding OTDM MIMO system based on singular value decomposition for 5G applications,” Applied Sciences (Switzerland), vol. 9, no. 13, 2019.

[8] S. E. Alavi et al., “Towards 5G: A Photonic Based Millimeter Wave Signal Generation for Applying in 5G Access Fronthaul OPEN,” Nature Publishing Group, 2015.

[9] X. Ge, H. Cheng, M. Guizani, and T. Han, “5G Wireless Backhaul Networks: Challenges and Research Advances,” 2014.

[10] F. Adachi, S. Member, and M. Sawahashi, “Decision Feedback Differential Phase Detection of W a r y DPSK Signals,” vol. 4, no. 2, pp. 203–210, 1995.

[11] A. Kanno et al., “16-QAM radio-over-fiber signal generation and its wireless transmission,” Optics Express, vol. 19, no. 26, pp. 56–63, 2012.

[12] T. Inoue and S. Namiki, “Carrier recovery for M-QAM signals based on a block estimation process with Kalman filter,” Optics Express, vol. 22, no. 13, p. 15376, 2014.

[13] X. Zhou, “Efficient clock and carrier recovery algorithms for singlecarrier coherent optical systems: A systematic review on challenges and recent progress,” IEEE Signal Processing Magazine, vol. 31, no. 2, pp. 35–45, 2014.

[14] A. Note, “Understanding Data Eye Diagram Methodology for Analyzing High Speed Digital Signals,” pp. 1–7, 2012.

[15] M. Gambhir and N. Shenvi, “Comparitive-Analysis-of-8-DPSK-and-16-QAM-Digital-Modulation-using-RoF-for-Hybrid-WDM-TDMPON.docx,” vol. 6, no. 6, pp. 189–193, 2015.